PCCP

ROYAL SOCIETY OF CHEMISTRY

COMMUNICATION

View Article Online
View Journal | View Issue

Cite this: *Phys. Chem. Chem. Phys.*, 2022, **24**, 4131

Received 15th November 2021,
Accepted 18th January 2022

DOI: 10.1039/d1cp05235g

rsc.li/pccp

Revisiting the plasmon radiation damping of gold nanorods†

Yanhe Yang,‡[a] Hao Xie,‡[ab] Jian You[a] and Weixiang Ye*[ab]

Noble metal nanoparticles have been utilized for a vast amount of optical applications. For applications that use metal nanoparticles as nanosensors and for optical labeling, higher radiative efficiency is preferred. To get a deeper knowledge about the radiation damping of noble metal nanoparticles, we used gold nanorods with different geometry factors (aspect ratios) as the model system to study. We investigated theoretically how the radiation damping of a nanorod depends on the material, and shape of the particle. Surprisingly, a simple analytical equation describes radiation damping very accurately and allows the disentanglement of the maximal radiation damping parameter for gold nanorods with resonance energy E_{res} around 1.81 eV (685 nm). We found very good agreement with theoretical predictions and experimental data obtained by single-particle spectroscopy. Our results and approaches may pave the way for designing and optimizing gold nanostructures with higher optical signal and better sensing performance.

Noble metal nanoparticles have a very large optical absorption and scattering cross-section owing to resonantly driven electron oscillations upon interaction with light, which is also known as particle plasmons.[1] Particle plasmons enable the nanoparticles to collect light energy efficiently and store it in the oscillation of the conduction electrons for tens of femtoseconds. Then, the plasmon energy is redistributed *via* several channels: interband, intraband, radiation, and surface damping.[2–5] Among these, the radiation damping (radiative energy loss of particle plasmons) quantifies the efficiency of the transformation of the plasmon oscillation energy into the emitted photons. It is well known that radiation damping scales with the volume of the nanoparticles and plays a dominant part in the overall damping of particle plasmons for large metal nanoparticles.[6,7] Radiation damping of a particle represents the efficiency of transformation of localized plasmons into propagating electromagnetic radiation. For the applications that used metal nanoparticles as nanosensors and optical labeling, higher radiative efficiency is preferred (higher optical signal).[8–12]

Historically, radiation damping is related to the volume of the nanoparticles, V, and the radiation damping parameter, κ_{rad}, according to $\Gamma_{rad} = 2\hbar\kappa_{rad}V$.[6] However, we noticed that such a description may have deviations for particles with different geometry factors. For example, for gold nanorods with different aspect ratios (ARs).[6,7,13] We have therefore revisited this problem and derived an analytical equation that accurately describes the radiation damping for gold nanorods. The derivation is based on the fundamental light scattering equation from Clausius–Mossotti, which uses the complex susceptibilities of the particle material and geometry factors as input.[14] Applying the theory to gold nanorods with different AR, we show theoretically and with experiments how the historical radiation damping parameter depends on the AR. Our results indicate that there is an optimal radiation damping parameter for gold nanorods with a certain AR. Such gold nanorods have plasmon resonance that corresponds to the minimal imaginary part of the dielectric function of gold. Intuitively, the minimal imaginary part of the dielectric function for a material corresponds to the minimal energy loss. Our results and approaches may pave the way for designing and optimizing gold nanostructure with higher optical signal and better sensing performance.

In this letter, we have chosen gold nanorods with different geometry factors (or ARs) as the model system to study. There are two reasons for this: recipes are available for making gold nanorods with good control of sizes and ARs, and they have dipole plasmon resonances in the visible light region of the spectrum which can be easily studied.[15] As mentioned above, one of the plasmon energy decay channels is radiative decay. The radiation damping of gold nanorods represents the efficiency to transform the collective electron oscillation energy into the optical far-field (see Fig. 1(a)). To determine the

[a] *School of Physical Science and Technology, Soochow University, Suzhou 215006, China. E-mail: wxy@hainanu.edu.cn*
[b] *Department of Physics, School of Science, Hainan University, Haikou 570228, China*

† Electronic supplementary information (ESI) available: Gold nanorod synthesis and characterization, SEM images of the gold nanorods, synthesis details and dimensions of the gold nanorods. See DOI: 10.1039/d1cp05235g

‡ Contributed equally.

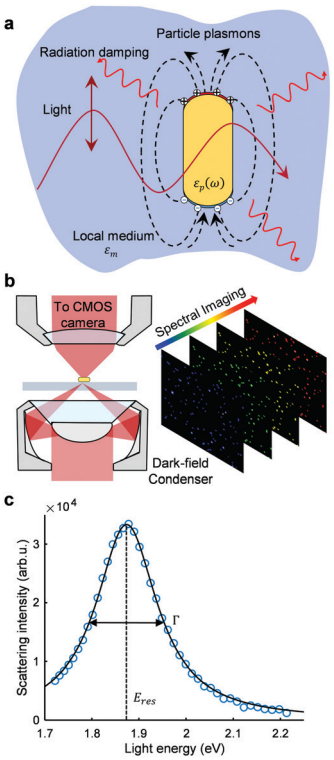

Fig. 1 Radiative decay of particle plasmons and single-particle darkfield scattering spectroscopy. (a) Schematic representation of the radiative decay of particle plasmons in the gold nanorods. The metal nanoparticle behaves as an optical dipole antenna under light excitation, which is able to transform the collective electron oscillation energy into the optical far-field. (b) The scattering spectrum of the gold nanorods can be obtained by using single-particle darkfield scattering spectroscopy. Here, we used the spectral imaging method to record the scattering spectrum of thousands of particles in the field of view simultaneously. (c) We can quantify the plasmon resonance energy (E_{res}) and linewidth (Γ) by fitting the recorded spectrum with a Lorentzian function.

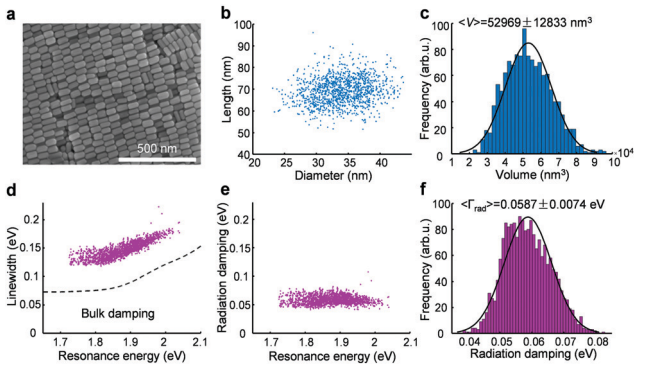

Fig. 2 We used the scanning electron microscope (SEM) and single-particle spectroscopy to correlate the mean volume and mean radiation damping of the same batch of gold nanorods. (a) Representative scanning electron microscopy (SEM) image of the gold nanorods used in this work. (b) We obtained the diameter (D) and length (L) of thousands of nanorods from the SEM images. (c) We calculated the particle volume (V) with these values (D, L) by modeling the gold nanorods as a spherically capped cylinder shape. The histogram shows the distribution of the nanoparticles' volume for around one thousand nanoparticles. (d) We measured the plasmon linewidth (Γ) of the same batch of gold nanorods with the single-particle darkfield scattering spectroscopy operating in the spectral imaging mode. Each pink dot represents the data obtained from one single nanoparticle. It is clear that Γ depends on the plasmon resonance energy (E_{res}), which follows a similar trend of bulk damping. (e) We extracted the radiation damping (Γ_{rad}) of each gold nanorod by subtracting the contribution of the bulk damping. The radiation damping does not have a strong dependency on the E_{res}. (f) The histogram shows the distribution of the Γ_{rad} for around two thousand nanoparticles.

radiation damping from the homogeneous plasmon line width (the overall plasmon damping) of the gold nanorods with high statistics, we used spectral imaging single-particle darkfield spectroscopy to collect the scattering spectrum of the particles. As shown in Fig. 1(b), we used an upright microscope equipped with a darkfield condenser and a liquid crystal tunable filter as our spectral imaging setup.[11] The scattered light of the gold nanorods under different wavelengths of excitation is collected by a CMOS camera. Such configuration allows us to record all the particles within the field of view (FOV) simultaneously. From the recorded scattering intensities at different wavelengths, we can obtain the plasmon resonance energy (E_{res}) and linewidth (Γ) with a Lorentzian function (see Fig. 1(c)).

The particles investigated here were produced wet-chemically. The gold nanorods have diameters from 29 to 92 nm and ARs from 1.6 to 2.8 (see Fig. S1 and Table S1, ESI†). Please note that the surface damping and chemical interface damping depend on the average distance of electrons to the surface, which gives negligible contributions to the total plasmon damping for the particles used in this work.[16,17] We have used a scanning electron microscope (SEM) and single-particle spectroscopy to correlate the mean volume and mean radiation damping of the same batch of gold nanorods. To achieve this, we first determined the diameter (D) and length (L) of thousands of nanorods from the SEM images (see Fig. 2(a and b)). Then, we calculated the particle volume (V) with these values (D, L) by modeling the gold nanorods as a spherically capped cylinder shape for every particle. The mean volume ($\langle V \rangle$) of one batch of the gold nanorods can be obtained by fitting the distribution of the nanoparticles' volume with a Gaussian function (see Fig. 2(c)). Subsequently, we measured the scattering spectrum of the same batch of gold nanorods with our spectral imaging setup and determined the total plasmon damping (Γ) for every particle (see Fig. 2(d)). It should be noted that the Γ depends on the plasmon resonance energy (E_{res}) due to the contributions of the bulk damping (interband and intraband damping) as nonradiative damping $\Gamma_{non\text{-}rad}$. The bulk damping of the dipole plasma resonance can be estimated by using the real part ε_1 and imaginary part ε_2 of the metal–dielectric function at resonance conditions as:[18]

$$\Gamma_{(non\text{-}rad)} = 2\varepsilon_2 \Big/ \left|\varepsilon_1{}'\right| \quad (1)$$

The $\Gamma_{non\text{-}rad}$ also depends on the E_{res} and shows an increasing trend for higher energy due to the contribution of interband damping (the dashed line in Fig. 2(d)). We can extract the radiation damping of each gold nanorod by subtracting the

contribution of the bulk damping from the total plasmon damping as $\Gamma_{\mathrm{rad}} = \Gamma - \Gamma_{\mathrm{non\text{-}rad}}$. It is clear that the radiation damping does not have a strong dependency on the E_{res} around the mean E_{res} of all the particles (see Fig. 2(e), 1.7 to 2 eV). The mean radiation damping $\langle\Gamma_{\mathrm{rad}}\rangle$ of the same batch of gold nanorods can be obtained by fitting the distribution of the Γ_{rad} for a thousand nanoparticles with a Gaussian function (see Fig. 2(f)). Finally, we are able to correlate the $\langle\Gamma_{\mathrm{rad}}\rangle$ to a certain $\langle V\rangle$ of the same batch of gold nanorods. We have repeated this procedure for all the batches of gold nanorods used in this work.

Before introducing our analytical equation for radiation damping, we have determined the mean radiation damping parameter $\langle\kappa_{\mathrm{rad}}\rangle$ from $\langle\kappa_{\mathrm{rad}}\rangle = \langle\Gamma_{\mathrm{rad}}\rangle/2\hbar\langle V\rangle$ for all batches of gold nanorods. Our experimental data follows this equation very well (see Fig. 3(a)) and the value $\langle\kappa_{\mathrm{rad}}\rangle = 6.55 \pm 0.02 \times 10^{-7}$ fs^{-1} nm^{-3} is in the same order as the previously reported values.[6,7] The small discrepancy may be due to the fact that they used gold nanorods with different ARs. The plasmon resonance wavelength or energy of a certain particle mainly depends on the geometry factor, which means that the $\Gamma_{\mathrm{non\text{-}rad}}$ and Γ_{rad} should rely on the geometry factor as well.

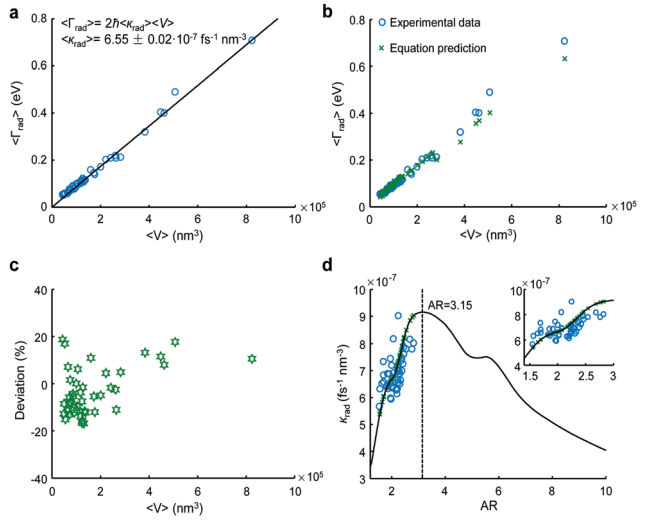

Fig. 3 Comparison of experimental data to our mathematical description for radiation damping of gold nanorods. (a) The radiation damping (Γ_{rad}) of gold nanorods follows a quasi-linear trend with the particle volume (blue dot). We determined the mean radiation damping parameter from the best linear fit. (b) Our mathematical predictions of the radiation damping of gold nanorods (green cross) follow the same trend as the experimental data by using the mean volume and mean AR from SEM images as input values. (c) The deviations of our mathematical predictions to the experimental data are below 20% for the different sizes of gold nanorods. (d) The radiation damping parameter is a function of particles AR. The blue dots and green crosses are experimental data and our mathematical predictions. The black line is the extrapolation by using gold nanorods with a constant diameter (20 nm) but a different AR (1.5 to 10). The experimental data and our mathematical predictions show the same dependency on AR. Our mathematical predictions indicate that there is an optimal radiation damping parameter for gold nanorods with an AR of around 3.15. Such gold nanorods have E_{res} around 1.81 eV (685 nm) which corresponds to the minimal point of the imaginary part of the dielectric function of bulk gold.

In our case, for gold nanorods we investigated how the radiation damping depends on AR. Therefore, we have revisited this problem and derived an analytical equation based on the fundamental light scattering equation from Clausius–Mossotti to describe the radiation damping for gold nanorods. The plasmon resonance of a nanoparticle is the frequency or wavelength where the polarizability α reaches a maximum. For particles with dimensions smaller than the wavelength of light, this polarizability is given by the Clausius–Mossotti equation (in the form of Richard Gans):[19]

$$\alpha = V\frac{\varepsilon_{\mathrm{p}} - \varepsilon_{\mathrm{m}}}{\varepsilon_{\mathrm{m}} + L(\varepsilon_{\mathrm{p}} - \varepsilon_{\mathrm{m}})} \tag{2}$$

Here, V is the particle volume, L is a geometry factor for the long axis that is approximately $1/L \approx (1 + \mathrm{AR})^{1.6}$ for nanorods,[12] ε_{m} is the dielectric function of the surrounding medium (in our case, is water), and $\varepsilon_{\mathrm{p}} = \varepsilon_1 + i\varepsilon_2$ is the particles' complex susceptibility (dielectric function) of gold. In metals, the real part of the particles' susceptibility ε_1 can be negative and, especially for coin and alkali metals, the imaginary part ε_2 comparatively small. As the dielectric function of the surrounding medium usually is positive, this leads to a strong maximum of polarizability at specific resonance energy (E_{res}) or resonance wavelength (λ_{res}). If ε_2 depends only weakly on wavelength, the polarizability has a maximum near the place where the real part of the denominator in eqn (2) is zero:

$$\Re\left(\left|\varepsilon_{\mathrm{m}} + L(\varepsilon_{\mathrm{p}} - \varepsilon_{\mathrm{m}})\right|\right) = 0 \tag{3}$$

Eqn (3) determines the resonance condition for the nanoparticles in a certain surrounding medium:

$$\varepsilon_1 = \varepsilon_{\mathrm{m}}\left(1 - \frac{1}{L}\right) \tag{4}$$

Combining eqn (2) and (4), we can express the polarizability at the resonance condition:

$$\alpha_{\mathrm{res}} = \frac{V}{L}\left(1 + \frac{i\varepsilon_{\mathrm{m}}}{L\varepsilon_2}\right) \tag{5}$$

The corresponding maximum cross sections for scattering and absorption C_{sca} and C_{abs} are:

$$C_{\mathrm{sca}} = \frac{k^4}{6\pi}|\alpha|^2\Big|_{\mathrm{at\ res}} = \frac{k^4}{6\pi}\cdot\frac{V^2}{L^2}\left(1 + \frac{{\varepsilon_{\mathrm{m}}}^2}{L^2{\varepsilon_2}^2}\right) \tag{6}$$

and

$$C_{\mathrm{abs}} = k\Im(\alpha)|_{\mathrm{at\ res}} = k\frac{V}{L^2}\cdot\frac{\varepsilon_{\mathrm{m}}}{\varepsilon_2} \tag{7}$$

Here, k is the wavevector and $k = \dfrac{2\pi\sqrt{\varepsilon_{\mathrm{m}}}}{\lambda_{\mathrm{res}}}$ at the resonance wavelength.

Combining eqn (2), (6), and (7), we obtained the analytical equation for radiation damping with the knowledge of the value of nonradiative damping, $\Gamma_{\mathrm{non\text{-}rad}}$ scattering cross-section, C_{sca}, and absorption cross-section, C_{abs}, at resonance

conditions:[20]

$$\Gamma_{\mathrm{rad}} = \left.\frac{C_{\mathrm{sca}}}{C_{\mathrm{abs}}}\right|_{\mathrm{at\ res}} \cdot \Gamma_{\mathrm{non\text{-}rad}} = \frac{4\pi^2}{3} \cdot \left(\frac{\sqrt{\varepsilon_{\mathrm{m}}}}{\lambda_{\mathrm{res}}}\right)^3 \cdot \frac{V}{L} \cdot \frac{L^2\varepsilon_2{}^2 + \varepsilon_{\mathrm{m}}{}^2}{L\varepsilon_2\varepsilon_{\mathrm{m}}} \cdot \frac{2\varepsilon_2}{\left|\varepsilon_1'\right|} \quad (8)$$

This equation can be further simplified by expressing the λ_{res} in an analytical form with the help of the Drude model. In this case, the dielectric function of the particle can be written as:[1]

$$\varepsilon(\omega) \approx \varepsilon_\infty - \frac{\omega_{\mathrm{p}}{}^2}{\omega^2} + i\frac{\omega_{\mathrm{p}}{}^2\gamma}{\omega^3} \quad (9)$$

Here, $\varepsilon_\infty = 9.84$ is the background permittivity which is used to correct the contribution of d-band electrons that are close to the Fermi surface, $\omega_{\mathrm{p}} = \sqrt{Ne^2/\varepsilon_0 m^*} = 9$ eV is the bulk plasmon frequency with effective electron mass m^* due to the band structure corrections, and $\gamma = 67$ meV is the damping of the free electrons.

To show how nicely the Drude model predicts the dielectric function of gold, we have plotted the real and imaginary parts of the dielectric function of bulk gold calculated using the above Drude parameters and experimental data measured by Johnson and Christy (JC) in Fig. S2 (ESI†). With the real part of the Drude dielectric function $\varepsilon_1 = \varepsilon_\infty - \omega_{\mathrm{p}}{}^2/\omega^2$ from eqn (9) inserted into the resonance condition, eqn (4), we can express the resonance wavelength as:

$$\lambda_{\mathrm{res}} = 2\pi c_0/\omega_{\mathrm{res}} = \lambda_{\mathrm{p}}\sqrt{\varepsilon_\infty + \varepsilon_{\mathrm{m}}\left(\frac{1}{L} - 1\right)} \quad (10)$$

where $\lambda_{\mathrm{p}} = 2\pi c_0/\omega_{\mathrm{p}}$ is the bulk plasmon wavelength and c_0 is the speed of light in a vacuum. Please note that this is the Eigen resonance wavelength of particle plasmons without any damping. We have plotted λ_{res} of gold ellipsoidal nanoparticles predicted by eqn (10) and calculated by quasi-static approximation (QSA) simulation in Fig. S3 (ESI†). The results from the equation are matched surprisingly well with the QSA simulation. In addition, to get a more precise resonance wavelength, one could add additional terms into the Eigen resonance wavelength obtained from the Drude model. One term is the retardation effects, the other term is the contribution interband transition.[13] However, those terms only have the phenomenological model. For the sake of simplicity, we did not include them in our equation. We also plotted λ_{res} of gold nanorods with the same size as we synthesized by boundary element method (BEM) simulation in Fig. S3 (ESI†), which follows the same trend as the QSA prediction.[21] But, the λ_{res} of gold nanorods shifts to the longer wavelength compared with the Eigen resonance wavelength for larger and longer particles.

Combining eqn (10) and (8), we reached the final analytical equation of radiation damping at the resonance condition:

$$\Gamma_{\mathrm{rad}} = \frac{8\pi^2}{3} \cdot \frac{1}{\lambda_{\mathrm{p}}{}^3(\varepsilon_\infty - \varepsilon_1)^{3/2}} \cdot \left(\varepsilon_2{}^2 + \frac{\varepsilon_1{}^2}{(L-1)^2}\right)\sqrt{\frac{L\varepsilon_1}{(L-1)\left(\left|\varepsilon_1'\right|\right)^2}} \cdot V \quad (11)$$

It is clear that the radiation damping of a plasmonic nanoparticle depends on the geometry factor of the particle L, the bulk plasmon wavelength λ_{p}, the dielectric function, and the material background permittivity ε_∞ of the material. Comparing our analytical equation with the historical expression $\Gamma_{\mathrm{rad}} = 2\hbar\kappa_{\mathrm{rad}}V$, we can obtain the analytical expression for the radiation damping parameter at the resonance condition:

$$\kappa_{\mathrm{rad}} = \frac{4\pi^2}{3\hbar} \cdot \frac{1}{\lambda_{\mathrm{p}}{}^3(\varepsilon_\infty - \varepsilon_1)^{3/2}} \cdot \left(\varepsilon_2{}^2 + \frac{\varepsilon_1{}^2}{(L-1)^2}\right)\sqrt{\frac{L\varepsilon_1}{(L-1)\left(\left|\varepsilon_1'\right|\right)^2}} \quad (12)$$

To show how precise the analytical equation of radiation damping for gold nanorods is, we have plotted our mathematical predictions of the radiation damping of gold nanorods (green cross) by using the mean volume and mean AR from SEM images as input values, and the experimental data obtained from single-particle spectroscopy in Fig. 3(b). The error bars for the radiation damping and volume of the particles have been omitted to avoid cluttering of the figure. The deviations of our mathematical predictions to the experimental data are below 20% for the different sizes of gold nanorods by using the experimental data as a reference (see Fig. 3(c)). We have noticed that the radiation damping parameter is a function of geometry factor from eqn (12), which means that the particles with different geometry factors (in our case, ARs) have different efficiency to transform the collective electron oscillation energy into the optical far-field. Therefore, we have plotted the radiation damping parameter as a function of nanorods' AR (see Fig. 3(d)). The blue dots and green crosses are experimental data and our mathematical predictions, respectively. The black line is the extrapolation by using gold nanorods with a constant diameter (20 nm) but different ARs (1.5 to 10). The experimental data and our mathematical predictions follow the same dependency on AR, which is first increased and then decreased. We also included the comparison with the BEM simulation in Fig. S4 (ESI†), which shows the same trend. However, both experimental data and BEM simulation demonstrate a lower value compared with the mathematical model for particles with larger AR and diameter, which is due to the increase of retardation effects. Interestingly, our mathematical prediction indicates that there is a maximal radiation damping parameter for gold nanorods with an AR of around 3.15. Such gold nanorod has E_{res} around 1.81 eV (685 nm) which corresponds to the minimal point of the imaginary part of the dielectric function of bulk gold (see Fig. S2, ESI†). In the picture of the particle plasmon, this

maximal point for radiation damping parameter may correspond to the minimal point of nonradiative damping, $\Gamma_{\text{non-rad}}$, due to the suppression of interband damping. This maximal radiation damping parameter should make gold nanorods with E_{res} around 1.81 eV become one of the best candidates in optical applications where a large optical far-field signal is required, such as single-particle biosensing.

Conclusions

In conclusion, we have investigated the radiation damping of particle plasmons in single gold nanorods and derived an analytical formula describing the radiation damping. We have shown that experimental data of radiation damping follows quite well the trend predicted by our theory. We have found a maximal radiation damping parameter for gold nanorods with resonance energy E_{res} around 1.81 eV (685 nm), which corresponds to the minimal point of the imaginary part of the dielectric function of gold. This finding indicates that gold nanorods with such resonance energy have relatively high light-scattering efficiencies and large optical far-field signals. A major advantage of the analytical equation of radiation damping is that it can be used to compare different nanoparticles: plasmonic particles of different materials and shapes, such as silver nanorods and silver spheres. We believe that our results and approaches could pave the way for designing and optimizing gold nanostructures with higher optical signals and better sensing performance.

Author contributions

W. Y. initiated and designed the research. W. Y. derived the mathematical models, constructed the microscope setup, gave guidance on the optical measurement, interpreted the data, performed data analysis, and wrote the manuscript text. Y. Y. and H. X. performed the single-particle characterization and SEM measurements. Y. Y., H. X., and J. Y. performed the gold nanorod synthesis and size characterization.

Conflicts of interest

There are no conflicts to declare.

Acknowledgements

W. Y. acknowledges the financial support by the National Natural Science Foundation of China (62105229), the Natural Science Foundation of Jiangsu Province (BK20200875), and the Natural Science Foundation of The Jiangsu Higher Education Institutions of China (20KJD150003) W. Y. thank Dr Weihai Ni from the Soochow University for providing the chemical resources and instruments for gold nanorod synthesis and Dr Carsten Sönnichsen from the University of Mainz for constructive discussions about particle plasmons during the last six years.

Notes and references

1 S. Carsten, *Plasmons in Metal Nanostructures*, Cuvillier Verlag Göttingen, 2001.
2 H. Hovel, S. Fritz, A. Hilger, U. Kreibig and M. Vollmer, *Phys. Rev. B: Condens. Matter Mater. Phys.*, 1993, **48**, 18178–18188.
3 B. Foerster, V. A. Spata, E. A. Carter, C. Sonnichsen and S. Link, *Sci. Adv.*, 2019, **5**, eaav0704.
4 S. A. Lee and S. Link, *Acc. Chem. Res.*, 2021, **54**, 1950–1960.
5 J. Olson, S. Dominguez-Medina, A. Hoggard, L. Y. Wang, W. S. Chang and S. Link, *Chem. Soc. Rev.*, 2015, **44**, 40–57.
6 S. Carsten, T. Franzl, T. Wilk, G. von Plessen, J. Feldmann, O. Wilson and P. Mulvaney, *Phys. Rev. Lett.*, 2002, **88**, 077402.
7 C. Novo, D. Gomez, J. Perez-Juste, Z. Zhang, H. Petrova, M. Reismann, P. Mulvaney and G. V. Hartland, *Phys. Chem. Chem. Phys.*, 2006, **8**, 3540–3546.
8 J. N. Anker, W. P. Hall, O. Lyandres, N. C. Shah, J. Zhao and R. P. Van Duyne, *Nat. Mater.*, 2008, **7**, 442–453.
9 S. Celiksoy, W. Ye, K. Wandner, F. Schlapp, K. Kaefer, R. Ahijado-Guzman and C. Sonnichsen, *J. Phys. Chem. Lett.*, 2020, **11**, 4554–4558.
10 R. Ahijado-Guzman, J. Prasad, C. Rosman, A. Henkel, L. Tome, D. Schneider, G. Rivas and C. Sonnichsen, *Nano Lett.*, 2014, **14**, 5528–5532.
11 W. Ye, S. Celiksoy, A. Jakab, A. Khmelinskaia, T. Heermann, A. Raso, S. V. Wegner, G. Rivas, P. Schwille, R. Ahijado-Guzman and C. Sonnichsen, *J. Am. Chem. Soc.*, 2018, **140**, 17901–17906.
12 S. Celiksoy, W. Ye, K. Wandner, K. Kaefer and C. Sonnichsen, *Nano Lett.*, 2021, **21**, 2053–2058.
13 B. Foerster, J. Rutten, H. Pham, S. Link and C. Sönnichsen, *J. Phys. Chem. C*, 2018, **122**, 19116–19123.
14 D. R. H. Craig and F. Bohren, *Absorption and Scattering of Light by Small Particles*, Wiley-VCH Verlag GmbH & Co. KGaA, 1998.
15 X. Ye, C. Zheng, J. Chen, Y. Gao and C. B. Murray, *Nano Lett.*, 2013, **13**, 765–771.
16 G. V. Hartland, *Chem. Rev.*, 2011, **111**, 3858–3887.
17 B. Foerster, *ACS Nano*, 2017, **11**, 2886–2893.
18 U. Kreibig, *Appl. Phys.*, 1976, **10**, 255–264.
19 R. Gans, *Ann. Phys.*, 1912, **342**, 881–900.
20 M. Z. Liu, M. Pelton and P. Guyot-Sionnest, *Phys. Rev. B: Condens. Matter Mater. Phys.*, 2009, **79**, 035418.
21 U. Hohenester, *Comput. Phys. Commun.*, 2012, **183**(2), 370–381.